Wind Driven Flow in the Mixed Layer Observed by Drifting Buoys during Autumn–Winter in the Midlatitude North Pacific

G. J. MCNALLY AND W. B. WHITE

Scripps Institution of Oceanography, La Jolla, CA 92093

(Manuscript received 2 July 1984, in final form 15 February 1985)

ABSTRACT

Wind-driven flow in the upper 90 meters during autumn–winter in the midlatitude North Pacific is investigated using satellite-tracked drifting buoys (i.e., drifters) deployed nearly simultaneously but drogued at different depths. The difference in the relationship between drifter velocity and wind stress as a function of drogue depth is observed to change when its drogue entered the deepening mixed layer. This change is characterized by a sudden increase in the amplitude of the near-inertial motions observed by the drifters and by the onset of a persistent net displacement whose downwind component is approximately 3 times as large as its crosswind component. Attempts to model this downwind flow as a windage result in a large unexplained residual downwind velocity component. On the other hand, 80–90% of the observed crosswind displacement is explained by an Ekman slab model (i.e., with flow uniform over the mixed layer). This large residual downwind velocity component combined with the Ekman driven crosswind component results in drifter displacements whose angle with respect to the forcing wind is significantly greater then 0° and significantly less than 45° to the right (i.e., ~30°).

Details of the flow obtained while the drogues were still below the deepening mixed layer suggests the presence of an Ekman-like spiral in the velocity vector beneath the mixed layer. Subsequent to all the drogues being in the mixed layer, the behavior of all the drifters with respect to the local wind stress vector was essentially the same (i.e. independent of their drogue depth).

1. Introduction

The launching of the Nimbus 6 satellite with its Random Access Measurement System (RAMS) in June 1975 provided the first relatively inexpensive means of remotely tracking small drifting buoys anywhere in the world's oceans. In following years use of this technique increased in the investigations into the nature of oceanic near-surface flow, which at that time was not normally sampled by the more conventional current meter moorings. A large number of these satellite tracked drifting buoys were deployed in such an investigation in the eastern midlatitude North Pacific as an element of the North Pacific Experiment (NORPAX) (Kirwan *et al.* 1978a,b, 1979). A more recent study of the data from these deployments showed that the near-surface flow was principally wind driven in the fall–winter seasons in this region. Further, this wind driven flow has a magnitude of approximately 1.5% of the surface wind speed and was directed approximately 30 degrees to the right of the surface wind vector (McNally, 1981). This latter study also suggested that the near-surface flow in the mixed layer was uniform with depth since the flow direction with respect to the local wind vector was the same for buoys which were drogued at 30 meters and those buoys which had reported the loss of their drogues. In August 1980, a deployment of 12 satellite tracked drifting buoys was made in an experiment designed to further investigate the vertical structure of wind-driven flow.

The twelve buoys were deployed in four groups of three buoys each. The groups were deployed at 35, 36, 37 and 38°N along 155°W. Each of the groups consisted of one drifter drogued at 30 meters, one at 60 meters and one at 90 meters. All of the drifters were identical to those used in the earlier NORPAX deployments except for the length of their drogue lines and the satellite system used to track them. In addition, the parachute drogues were smaller than those used in the previous studies, 4.3 m versus 8.5 m diameter in the previous studies. A description of these drifter systems can be found in McNally *et al.* (1978). The earlier deployments were tracked by means of the Random Access Measurement System (RAMS) while those of this most recent deployment were tracked by ARGOS. The ARGOS system offers two advantages over the older RAMS. First, ARGOS is serviced by two satellites instead of one, thus providing twice the number of RAMS fixes per day. Second, the ARGOS system provides position fixes with a rms error of ±1 km compared to the ±5 km rms position error of RAMS.

As an aid in interpreting the buoy displacements, synoptic surface wind vectors over the region were obtained from Fleet Numerical Ocean Center (FNOC).

These were used to compute wind stress vectors using the standard bulk formula (Fissel *et al.*, 1977). In addition, expendable bathythermograph (XBT) temperature profiles of the upper 400 m collected by the TRANSPAC ship-of-opportunity program, (White and Bernstein, 1979), were used to provide a time history of the near-surface temperature structure.

The raw ARGOS drifter positions, which are irregularly spaced in time, were interpolated to obtain four positions per day at the synoptic reporting times (0000, 0600, 1200 and 1800 GMT). The FNOC synoptic surface wind stress vector components were then interpolated to these drifter positions forming a joint drifter/wind stress dataset. TRANSPAC XBT data within 250 kilometers of drifters were used to construct an irregularly spaced time series of the depth of the surface mixed layer in the region of the drifter trajectories. The joint dataset of surface wind stress and drifter location, together with the time history of the mixed layer depth, are used in a study of the relationship between the flow in the upper 90 meters and the local surface wind stress and how this relationship is modified by the depth of the surface mixed layer.

2. General description of drifter movement

The most general description of the drifters' behavior is afforded by their composite trajectories (Fig. 1), which shows that the behavior of the drifters deployed at 36, 37 and 38°N to have been essentially the same. These trajectories describe an initial north–south meander followed by an eastward zonal displacement to ~150°W; thereafter their movement was northeastward. Trajectories of the group deployed at 35°N were also characterized by an initial north–south meander, followed by eastward zonal motion. The trajectories of the latter drifters did not turn to the northeast as was true for those drifters deployed north of 35°N. The trajectories in Fig. 1 reveal no systematic arrangement by drogue depth. Thus, on the large time and space scales implicit in Fig. 1 the behavior of drifters drogued at different depths was the same.

Since the relationship between the near-surface flow and surface wind stress was the principle objective of this study, a more meaningful way of presenting the drifter movements was in the coordinate system determined by the surface wind stress. Drifter velocities were rotated every six hours to obtain the drifter velocity components normal to the wind stress direction and parallel to it, with positive components 90° to the right of the wind and downwind respectively. A composite displacement plot of all the drifters in downwind–crosswind space is shown in Fig. 2. This figure was generated by initializing each drifter at 0, 0 and, then, advancing it in the downwind–crosswind direction using the 6 hourly downwind–crosswind drifter velocity components. The similarity of drifter behavior is even more apparent in this figure than in Fig. 1. The apparent difference in behavior of the

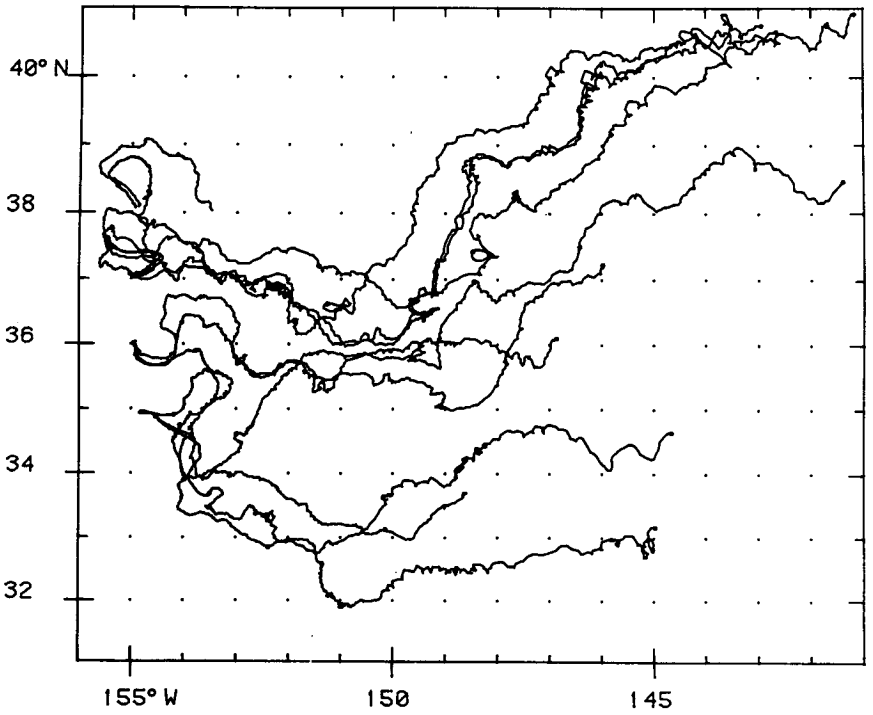

FIG. 1. Composite trajectories of four groups of three drifters each deployed along 155°W at 35, 36, 37 and 38°N on 28 August 1981.

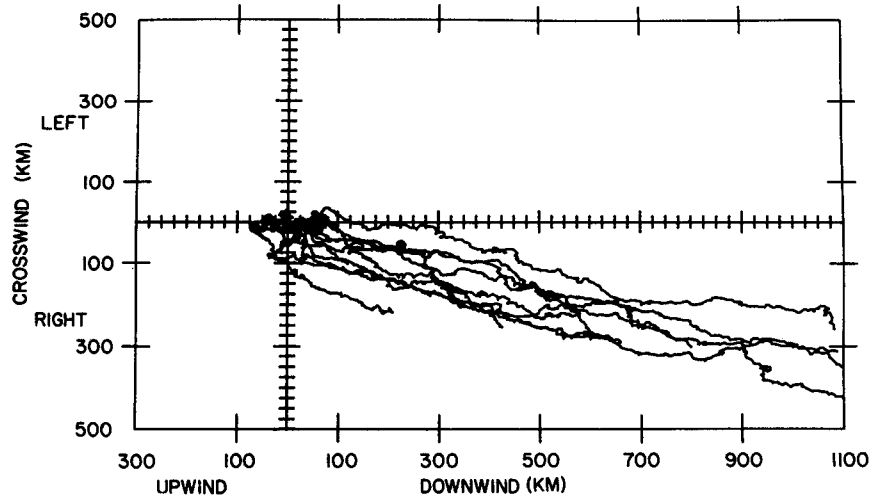

FIG. 2. Composite trajectories of the drifters in Fig. 1 shown in a downwind–crosswind coordinate system.

drifters deployed at 35°N, compared to those deployed north of 35°N, noted earlier in Fig. 1, is no longer seen, indicating that this difference was in fact due to spatial variability of the wind field.

A downwind displacement considerably larger than the crosswind (to the right of the wind) displacement is indicated by all of the drifters in Fig. 2, yielding an angle $\sim 20°$ to the right of the wind. Again there is no clear stratification by drogue depth in evidence.

3. Detailed description of the drifter group deployed at 37°N

Having seen that the behavior of drifters with respect to the local wind stress vector on these large time and space scales was essentially the same for each of the groups deployed, we selected one group (i.e., those deployed at 37°N) and examined its behavior in greater detail. Six hourly downwind–crosswind velocity components for each of these drifters were used to form downwind–crosswind displacements from deployment location as a function of time after deployment. A plot of the results of this calculation (Fig. 3, top panel) shows remarkably similar slopes for the time rate of downwind displacement for the three drifters over most of their records. However, the onset of this quasi-constant rate of downwind displacement occurred at a different time for each of the drifters, i.e., first for the 30-meter drogue drifter in mid-September, next for the 60-meter drogued drifter in early October, and finally for the 90-meter drogued drifter in late October. A similar delay is seen for the onset of crosswind displacements (Fig. 3, middle panel). The large spatial scales of the atmospheric forcing coupled with the relatively small separations of the three drifters results in almost identical wind stress at the three drifter locations. The 6 hourly wind stress at the 90 m drogued drifter is shown in Fig. 3, bottom panel. It should be noted that wind forcing events in excess of 4 dyn cm^{-2} occurred during the period when the deeper drogued drifters show little downwind displacement. Therefore it was not for lack of wind that these drifters did not move in downwind–crosswind directions, but rather as will be shown, when their drogues were deeper than the mixed layer depth.

As stated earlier, the ARGOS system used to track these drifters provided, on average, eight positions per day for each drifter with a rms accuracy of 1 kilometer. These positions, when interpolated to provide four estimates of velocity per day, resulted in

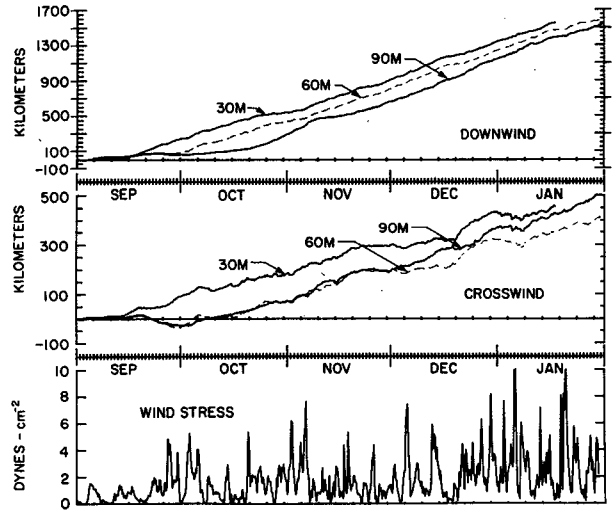

FIG. 3. (Upper panel) Downwind displacement versus time for the 30-, 60- and 90-meter drogued drifter deployed at 37°N. (Middle panel) Crosswind displacement versus time for the same drifters. (Lower panel) Local wind stress at the 90-meter drogued drifter.

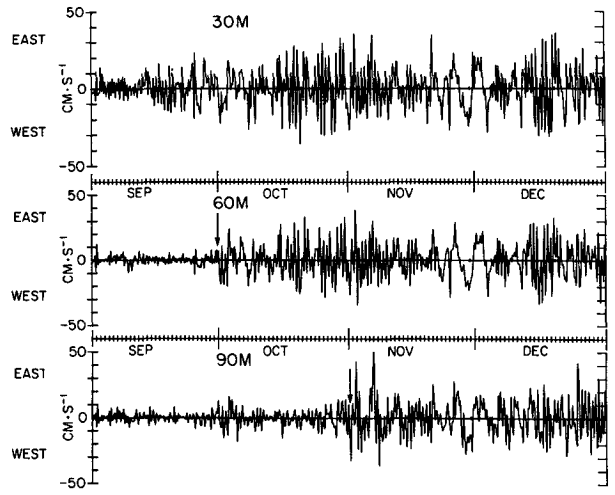

FIG. 4. (Upper panel) East–west (U) component of velocity is cm s^{-1} of 30-meter drogued drifter deployed at 37°N. (Middle panel) As in upper panel but for the 60-meter drogued drifter deployed at 37°N. (Lower panel) As in upper panel but for the 90-meter drogued drifter deployed at 37°N.

time and space sampling adequate to allow for the detection of near-inertial motions in the drifter movements, since the inertial period at 37°N is approximately 19 hours. A sample of the 6 hourly estimates of the zonal component of drifter velocity of the three drifters under discussion are shown in Fig. 4. These records are typical of drifter velocity records of the entire group and indicate the degree that drifter velocities were dominated by high frequency variability, which spectral analyses have shown to have been of near-inertial period. Examination of the records in Fig. 4 also indicate a clear time lag in the appearance of these strong near-inertial motions in the two deepest drogued drifters (i.e. 60 and 90 m). The initial appearance of these motions is indicated by arrows in the middle and bottom panels of Fig. 4. It should be noted that these times which mark the initial appearance of the near-inertial motions are at the same times, noted earlier, for the initial appearance of persistent downwind–crosswind displacements (Fig. 3).

The relative magnitude of near-inertial motions observed in drifter velocities is estimated from the comparison of the variance preserving plots of the spectra of the zonal component of velocity of the 30- and 90-meter drogued drifters. These spectra were computed for the months of October and December and shown in Fig. 5. The energy contained in the near-inertial peak of the 90-meter drogued drifter was clearly less than that of the 30-meter drogued drifters in October, (Fig. 5, upper panel), while the two peaks were essentially the same in December, (Fig. 5, lower panel). An estimate of the relative energetics of the near-inertial motions in each of velocity records of the three drifters is given in Table 1, listing the ratios of the spectral estimates at the near-inertial peak of the 60- and 90-meter drogued drifters to those of the 30-meter drogued drifter obtained from monthly spectra for the period September through January. These ratios find the 60- and 90-meter drogued drifters with only 35% of the inertial energy of the 30-meter drogued drifter in September. By October and throughout the balance of the record the 30- and 60-meter drogued drifters have comparable inertial energy. The inertial energy of the 90-meter drogued drifter increased in October to 42% and in November to 82% of that of the 30-meter drogue drifter. In December and January the inertial energy of all three drifters was comparable.

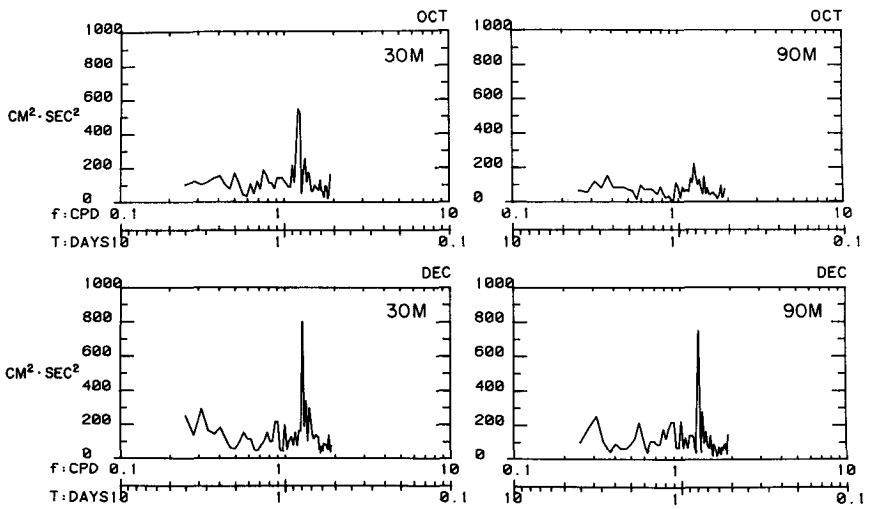

FIG. 5. (Upper panel) Variance conserving plots of the spectral energy density of the U component of the 30-meter drogued drifter (left) and 90-meter drogued drifter (right) deployed at 37°N for the month of October. (Lower panel) As in the upper panel but for December.

TABLE 1. The ratio of the monthly estimates of kinetic energy density at the inertial peak of the 60- and 90-meter drogued drifters, I_{60}, I_{90} respectively to that of the 30-meter drogued drifter I_{30}.

	I_{60}/I_{30}	I_{90}/I_{30}
Sep	0.35	0.35
Oct	1.15	0.42
Nov	1.13	0.84
Dec	0.94	1.01
Jan	1.03	0.96

These three drifters underwent a radical change in behavior during the early portion of the six months record under discussion. This change is characterized by the sudden increase in magnitude of the near-inertial motions and by the sudden onset of persistent downwind–crosswind displacements. Furthermore, this marked change in behavior occurred at successively later times for increasingly deeper drogued drifters. The time history of the depth of the surface mixed layer determines the relationship between drogue depth and mixed layer depth as it pertains to these abrupt changes in drifter behavior. The irregularly spaced time history of the depth of the surface isothermal depth for the period September through January, (Fig. 6), was constructed by giving equal weight to all TRANSPAC XBT traces taken within a 250 kilometer radius of the drifters. Using the dates marking the abrupt change in behavior noted earlier (i.e., 15 September, 1 October and 1 November for the 30-, 60-, and 90-meter drogued drifters, respectively) the mixed layer at these times was at a depth of 25, 50 and 72 meters, respectively. The 30-, 60- and 90-meter notation used to identify the drifters referred to the lengths of their drogue lines. Since the drogues were not equipped with pressure sensors at the end of their lines, the actual depths of the three drogues is not known. If it can be assumed that the dates noted earlier mark the times when the mixed layer reaches the actual depths of the drogues, then the actual drogue depths would have been approximately 80% of length of the drogue lines. Considering the magnitude of the working loads associated with near-inertial oscillation velocities in excess of 50 cm s^{-1} a drogue line shape that results in the depth of its drogue end being 80% of the line length does not seem unreasonable. Therefore, it is concluded that the observed change in drifter behavior does indeed mark the time that the mixed layer depth reached that of the drogue.

4. Comparison of observed flow and model flow

Having described the drifter data and its relationship to local surface wind stress and surface mixed layer depth, the following models are tested in an explanation of observations.

Model crosswind velocities are based upon the Ekman slab model (Davis *et al.*, 1981). This model is based upon the assumption that no change exists in magnitude or direction of the wind-driven flow within the mixed layer. It further assumes no wind-driven flow below the mixed layer. The characteristic of this model's wind driven flow is that it is directed 90° to the right of the surface wind stress with a magnitude of

$$V_E = |\tau| f/H \qquad (4.1)$$

where $|\tau|$ is the magnitude of the total wind stress vector in dyn cm^{-2}, f the Coriolis parameter, and H the mixed layer depth in meters. The mixed layer depth information in Fig. 6 is now fit with a line determined by linear regression for the period September through January and used to obtain 6 hourly mixed layer depths. Using these estimates of H and the 6-hourly surface wind stress data, the model crosswind velocity component V_E is calculated from (4.1) every 6 hours. Of course, this calculation ignores the transient effects of wind-driven flow generation, but these effects are small when dealing with the time-integrated velocity (i.e., net displacement).

Due to the smaller sized parachutes used in this deployment the downwind velocity component V_D is assumed to be the result of the direct forcing of the surface wind on the portion of the drifter hull above the ocean surface, a measure of drag commonly referred to as windage. A static balance of forces is assumed to exist, such that

$$V_D^2 \rho_w C D_w A_w = V_a^2 \rho_a C D_a A_a \qquad (4.2)$$

where the subscript a denotes air and the subscript w denotes water. The drag coefficients CD_a and CD_w are assumed equal to 1, so that

$$V_D = V_a \left(\frac{\rho_a A_a}{\rho_w A_w} \right)^{1/2}. \qquad (4.3)$$

For the area exposed to the wind, A_a the cross-sectional area of the cylindrical hull above the water line is used, which is nominally 1 meter below the top of the hull. The submerged drag area is composed of the submerged portion of the hull, the drogue line and the drogue itself. Again using FNOC's 6 hourly surface wind velocity, interpolated to each drifter's

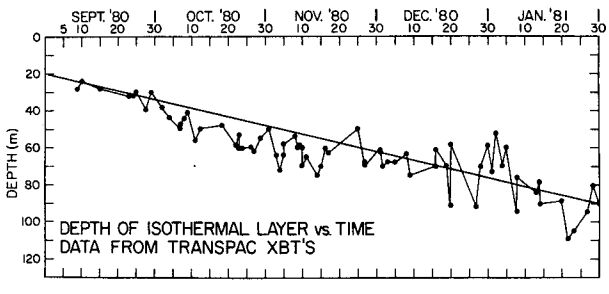

FIG. 6. Estimates of the mixed layer depth from TRANSPAC XBTs within 250 km of the drifters deployed at 37°N.

position, a windage velocity V_D was calculated for each drifter every 6 hours.

The trajectories of the three drifters' plotted in downwind–crosswind space (Fig. 7, left panel) are characterized by total downwind–crosswind displacements of approximately 1500 and 500 kilometers respectively. The calculated windage velocity V_D, properly modified to reflect the different drogue line lengths, was subtracted from the observed downwind velocities over the entire record. The results of this correction are seen in Fig. 7 (middle panel), revealing the degree to which this windage model fits the observations (Fig. 7, left panel). After removing the windage model velocities from the observed downwind velocities, a 900-kilometer downwind displacement remains in all three drifters' trajectories. In the process of reducing the observed downwind displacements, the trajectories are directed approximately 10° farther to the right of the wind than those of the uncorrected data [i.e., from ~20° to the right of the wind stress vector (Fig. 7, left panel) to 30° to the right of the wind stress vector (Fig. 7, middle panel)]. Though unsuccessful in explaining all of the observed downwind displacement, the windage correction brings these observations into agreement with those of previous deployments which were all ~30° to the right of the wind.

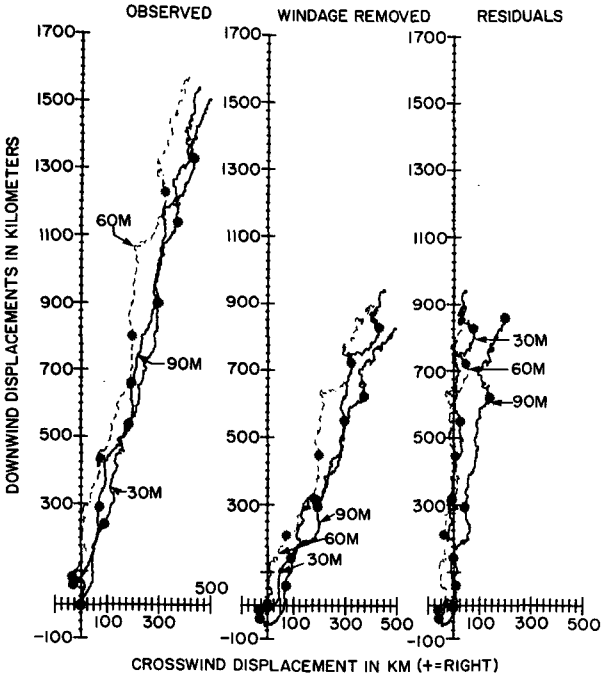

FIG. 7. The trajectories of the 30-, 60- and 90-meter drogued drifters deployed at 37°N in downwind–crosswind coordinate system. (Left panel) Using observed velocities. (Middle panel) After correcting the downwind velocity for windage. (Right panel) Using residual velocities after subtracting both windage and Ekman slab model velocities from the observed downwind and crosswind velocities respectively.

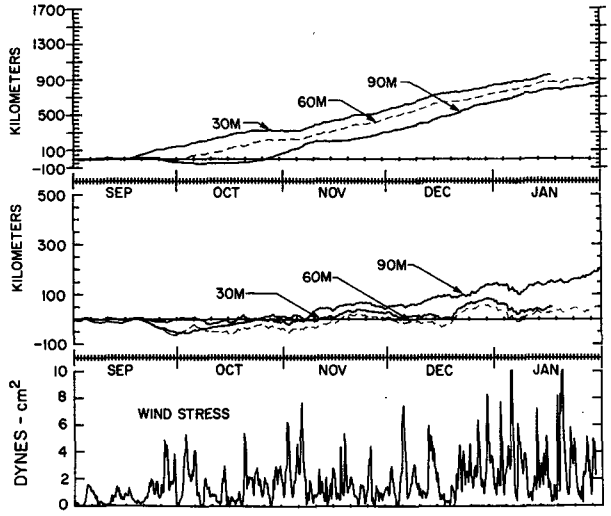

FIG. 8. Residual downwind displacement versus time for the 30-, 60-, and 90-meter drogued drifters deployed at 37° North. The residual downwind displacements (top panel) after removing model windage velocities from the observed downwind velocities (lower panel) The residual crosswind displacements after removing the Ekman slab model velocities from the observed crosswind flow. (Lower panel) Local wind stress at the 90-meter drogued drifter.

The modeled crosswind component V_E was not subtracted from the observed crosswind flow until after the drifter's drogue appeared to have entered the mixed layer. The dates used to mark the entry of the drogues into the mixed layer were those identified earlier; 15 September, 1 October and 1 November for the 30-, 60-, and 90-meter drogues, respectively. However, prior to those dates a significant portion of the drifter system, namely, the submerged portion of the hull and that portion of the drogue line in the mixed layer, were subjected to V_E. Therefore, during these periods a fraction of the crosswind flow equal to V_E, modified by the square root of the ratio of the drag area in the mixed layer to the drag area of the fouled parachute, was subtracted from the observed crosswind flow. Residual velocity components were obtained by subtracting the windage and Ekman slab model velocity components from observed downwind and crosswind velocity components, respectively. Trajectories of the drifters formed using these residual velocities are shown in Fig. 7 (right panel). Comparison of these trajectories to those uncorrected (left panel of Fig. 7) shows qualitatively how well the Ekman slab model fits the observed crosswind velocity data; i.e., it can be seen to have almost completely eliminated the observed crosswind component.

These residual displacements are seen in greater detail in Fig. 8 where the downwind (Fig. 8, top panel) and crosswind (Fig. 8, middle panel) residual displacements are plotted as a function of time. Comparison of Fig. 8 (top panel) and the observed downwind displacement in Fig. 3 (top panel) shows

that windage accounted for approximately 40% of the observed downwind displacement. In addition, removing this estimate of windage results in the drifters moving upwind to varying degrees prior to the time the drogues enter the mixed layer (indicated by arrows). After the drifter's drogues entered the mixed layer, the plots are quite similar.

The plots of residual crosswind displacement versus time (Fig. 8, middle panel) clearly indicates the success of the Ekman slab model in simulating the crosswind velocity. The residual crosswind displacements of the 30- and 60-meter drogued drifters were less than 15 km over the entire record, as opposed to 400 km the uncorrected displacements (Fig. 3, middle panel). The residual crosswind displacement of the 90-meter drogue drifter, while significantly smaller than the uncorrected, exhibited a trend not seen in either the 30- or 60-meter residual crosswind displacements. This plot also reveals cyclic behavior not observed in the downwind residual displacements. The most notable of these events occurs in all three drifters beginning in mid-December and ending early in January. The marked increase and subsequent decrease in residual crosswind displacements indicates that the Ekman slab flow model first underestimated and then overestimated the observed crosswind flow. A deepening and shallowing of the mixed layer depth, which is not accounted for in our assumed smooth monotonic increase in mixed layer depth, could account for these events. The XBT estimates of mixed layer depth in Fig. 6 suggests that this was the case. Notice the deepening of the mixed layer, that occurred about 20 December, was followed by a shallowing that persisted through early January.

Observed and residual downwind and crosswind displacements are summarized by month in Table 2, providing a more quantitative assessment of how successfully the observed displacements were modeled. An overall reduction in downwind displacement between 37 and 42% was achieved by removing the estimated windage. A seemingly obvious way to further reduce the large residual downwind displacements would have been to increase the estimates of windage by assuming some degree of drogue fouling. However, examination of the autocorrelations and cross-correlations of the total wind stress and the downwind and downwind residual velocities shown in Fig. 9 suggests that this is not appropriate.

Autocorrelations of wind stress and downwind (and downwind residual) velocities (Fig. 9, top and middle panel, respectively) reveal a characteristic time scale for the wind forcing of approximately 24 hours. The characteristic time scale, 5 hours, in both the downwind and residual downwind velocities is that of damped near-inertial motions which persist for approximately three inertial periods (i.e. 57 hours). Cross-correlation of the wind stress with both the downwind and downwind residual velocities provides relatively small values at zero lag (Fig. 9, lower panel). This is not surprising since there existed a basic mismatch between the time scales of variability in the wind stress and those in the downwind velocities. The sample correlation functions in Fig. 9 were not computed from the entire record, but for a period, (i.e., January) when the number of wind events was large, and the statistics seemed quasi-stationary (i.e. no trends, no change in variance with time). During January, 16 separate wind stress events occurred, each with maximum winds in excess of 15 m s^{1}. Examination of the cross-correlation in Fig. 9 (lower panel), reveals that not only did the downwind velocity component lag the wind by 6 to 12 hours, it also had an assymmetric character indicating that this component of velocity had a "memory" of $\sim$1.5 days. The cross-correlation of the wind stress and downwind residual velocity reveals that in removing the windage in the latter, the cross-correlation at zero lag was reduced to zero, while incurring only a slight reduction in the peak of cross-correlation estimate at the lag of approximately 6 hours. The lack of cross-correlation at zero lag for the downwind residual velocity implys that, indeed, that portion of the downwind velocity, directly forced by the surface wind on the hull, has been removed. The time lag and memory indicated by the cross-correlation of wind and residual downwind velocity are not characteristics that would be

TABLE 2. The downwind (DW), downwind residual (DWR), crosswind (CW), and crosswind residual (CWR) displacements in kilometers for the months of September through December and their totals for the entire period for each of the three drifters. The percent (%) of the total displacements explained by windage [1 − (DWR/DW)] × 100% and an Ekman slab model [1 − (CWR/CW)] × 100% for each drifter.

	30 m		60 m		90 m		30 m		60 m		90 m	
	DW	DWR	DW	DWR	DW	DWR	CW	CWR	CW	CWR	CW	CWR
Sep	250	140	90	41	60	−50	90	0	−50	−60	−40	−55
Oct	300	180	260	233	280	125	90	−10	110	20	100	65
Nov	390	230	450	235	350	225	120	35	140	40	140	40
Dec	415	275	450	280	385	325	125	35	125	40	175	90
Total	1355	825	1250	789	1075	625	425	60	325	40	375	140
(%)	39		37		42		86		88		62	

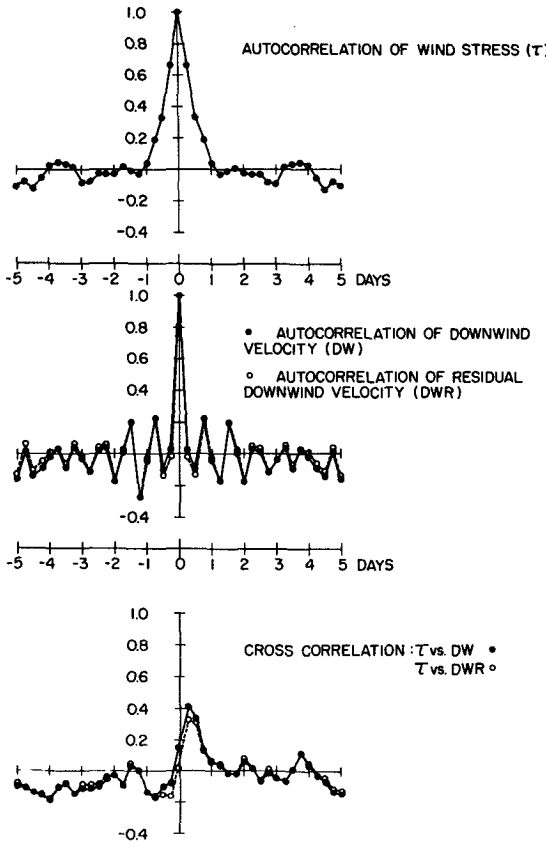

FIG. 9. Autocorrelation of the wind stress (top panel) and downwind (⊕) and downwind residual (○) (middle panel). Cross correlation of wind stress with downwind (⊕) and downwind residual velocities (○) for the 90 meter drogued drifter deployed at 37°N using the January drifter and wind data.

associated with windage. Thus, further reduction in the downwind residual velocity by simply increasing the windage estimate was not sensible, and the large downwind residual velocity remains as yet unexplained.

The summary of monthly crosswind displacements in Table 2 demonstrates that the Ekman slab model of wind driven flow, 90° to the right of the wind, was much more successful in explaining the observed crosswind displacements than windage was in explaining the observed downwind displacements. Percentages of 86, 88 and 62% of the total observed crosswind displacements of the 30-, 60- and 90-meter drogued drifters respectively were explained by the Ekman slab model. As with the downwind residuals, the crosswind residuals had a trend of increasing residual from September through December. Since both model velocities, (i.e. windage and Ekman slab), are directly proportional to the wind speed, which increased in intensity during this period, the most likely explanation for these trends is that the FNOC surface winds underestimated the real winds. The suggestion of such an underestimation is consistent with smoothing that must of necessity be part of the FNOC surface wind analyses. Further, Friehe and Pazan (1978) compared FNOC surface winds with direct measurements made in this region, finding that during strong wind events the FNOC surface winds were underestimated by ~20%.

The monthly displacements and the angle between these displacements and the local wind stress vector are summarized in Table 3 for (i) the raw observations, (ii) after removing the windage, and (iii) after removing both the Ekman slab model velocities and windage (i.e., residuals). The raw monthly displacements and their angles (Table 3) provide a quantitative assessment of the similarity of behavior of the drifters. It is only for the month of September that a significant difference is apparent when the 60- and 90-meter drogued drifters have significantly smaller displacements than the 30-meter drogued drifter and are directed to the *left* of the surface wind. After September, the monthly displacements of all three drifters increase with time and their angles remain relatively constant ~17° to the right of the wind. Removing the model windage velocities from the observed downwind velocities (Table 3b) resulted in an enhancement of the difference in behavior in September. Further, in October, this correction resulted in the 90-meter drogued drifter displacement, now the smaller of the three being directed ~15° further to the right of the wind than that of the corrected 30-meter drogued drifters displacement. Thereafter, the

TABLE 3. The monthly displacements (D) in kilometers and the angle of the displacement with reference to the wind direction (ϕ) for (*a*) the uncorrected data, (*b*) the observations corrected for windage and (*c*) the residuals after removing windage and the estimated crosswind flow from the observations.

	30 m		60 m		90 m	
	D (km)	ϕ (deg)	D (km)	ϕ (deg)	D (km)	ϕ (deg)
			a. Observed			
Sep	270	19	103	−29	72	−34
Oct	313	17	282	23	297	20
Nov	408	17	471	17	376	20
Dec	433	17	467	16	422	24
			b. Corrected for windage			
Sep	172	35	65	−51	56	−27
Oct	197	24	259	28	160	39
Nov	260	27	255	26	253	27
Dec	302	24	306	26	362	26
			c. Residuals			
Sep	140	0	64	−39	74	−132
Oct	180	−3	233	5	140	27
Nov	232	8	238	10	228	10
Dec	277	7	283	8	337	15

generally smaller windage corrected displacements are ~27° to the right of the wind (i.e., 10° farther to the right of the wind then the raw data).

The residual displacements of the 60- and 90-meter drogued drifters and their angles (Table 3c) indicate an increase in *upwind* component with drogue depth in September and significant crosswind flow not accounted for by the Ekman slab model which is limited to the mixed layer. Thereafter the 30- and 60-meter drogued drifters residual displacement are directed <10° to the right of the wind (i.e., essentially downwind). The October 90-meter drogued drifter residual displacement as directed at an angle 27°, which is significantly larger than those of the 30- and 60-meter drogued drifters (~3° and 5° respectively) once again indicating that a significant fraction of its observed crosswind velocity has not been accounted for by the Ekman slab model.

In conclusion, the observations of wind-driven flow within the mixed layer are characterized by a persistent downwind displacement recorded by all of the drifters when their drogues were contained within the mixed layer. A theoretical investigation into the nature of mixed layer dynamics that might lead to an explanation of this observation is outside the scope of this paper. However, the results of a recent study of the upper ocean response to a moving hurricane (Price, 1983) suggest a possible explanation of persistent downwind displacements. In his study, Price concluded that a rapid baroclinic response to the atmospheric forcing gave rise to significant and persistent downwind flow in the mixed layer. While it is true that the atmospheric wind stress events recorded in the present study region did not approach hurricane intensity, they were strong and occurred with rapid frequency. During January, for instance, 16 separate events with wind speeds of 15 m s^{-1} or greater occurred. Thus the persistent downwind displacements recorded by the drifters may represent the integrated effect of the type of oceanic response detailed in the Price study.

5. Flow beneath the mixed layer

The deeper drogued drifters provided observations of the flow beneath the mixed layer during the time periods when the depth of their drogues exceeded the mixed layer depth (i.e. September and September–October for the 60- and 90-meter drogued drifters, respectively). These data were used in an investigation of the characteristics of the velocity as a function of depth below the mixed layer and its relationship to local wind stress.

Five-day, vector-averaged velocities were used in this investigation in order to remove the small near-inertial motions of the drifters (see Fig. 4). Again, assuming this sub-mixed layer flow is related to the local wind stress, the downwind and crosswind components of the 5-day average velocities were formed. The windage component was removed from the downwind component and a portion of Ekman slab model was removed from the crosswind flow. The plot of the residual velocities in a wind coordinate system is shown in Fig. 10 for both the 60-m and 90-m drogued drifters. The vectors are numbered in chronological order, which owing to mixed layer deepening, is on order to decreasing depth beneath the mixed layer. The velocity hodograph produced by joining the end points of these vectors suggests that the flow beneath the mixed layer decreased in magnitude and turned, in a clockwise direction, farther to the right of the surface wind stress vector with increasing depth beneath the mixed layer (i.e., in qualitative agreement with an Ekman spiral). Rapid deepening of the mixed layer around 1 October (see Fig. 6) abruptly truncated that portion of the spiral recoverable from the 60-meter drogued drifter. However, during the time that its drogue was beneath the mixed layer, the 60-meter drogued drifter had a velocity vector that was consistently at a smaller angle to the right of the surface wind vector than that of the deeper 90-meter drogued drifter. The 90-meter drogued drifter provided a more complete realization of the behavior of velocity as a function of depth below the mixed layer because of the decrease in the rate of mixed layer deepening below 60 m.

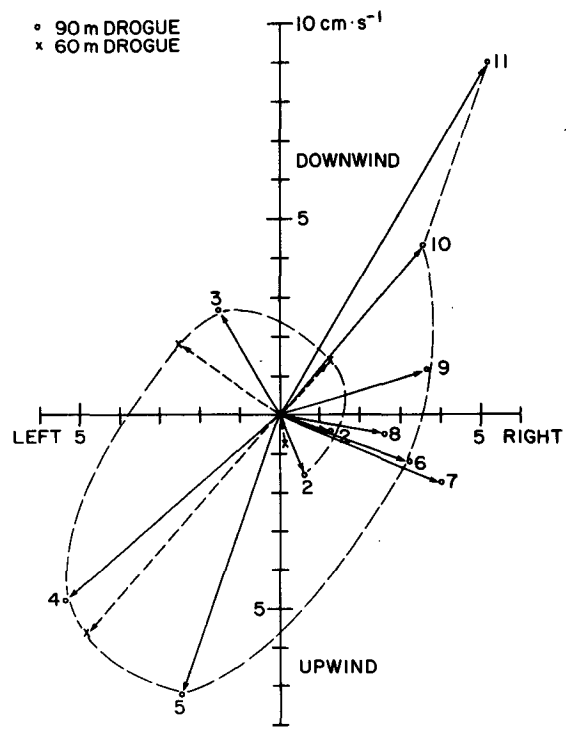

FIG. 10. 5-day vector averaged velocities for the 60 meter (cross) and 90 meter (circle) drogued drifter deployed at 37°N [plotted in a wind coordinate system].

The fact that the TRANSPAC XBT data do not provide a detailed time history of the behavior of the mixed layer deepening at the drifter location, coupled with the uncertainty of the actual drogue depth, combine to preclude a more detailed description of the behavior of the velocity below the mixed layer (i.e., *e*-folding depth, rate of turning with depth).

6. Summary and conclusions

Data from a multi-drogued depth drifter deployment in the midlatitude North Pacific were used to investigate wind driven flow in the mixed layer during the autumn–winter season. Since the major focus of this study is the relationship between the near-surface flow and the surface wind, the drifter data was studied with respect to the surface wind stress vector and presented in a wind coordinated system (i.e. downwind–crosswind components). In addition, displacements rather then velocities were used so that the underlying mean wind-driven flow could be readily observed in the presence of the larger velocities of the near-inertial motions.

The rapid seasonal deepening of the mixed layer in this region results in all of the drifter's drogues (i.e. 30-, 60- and 90-meters) being exceeded by the mixed layer depth by 1 November, two months after their deployment. Thereafter, data from all drifters indicate a persistent wind-driven flow at ~20° to the right of the wind stress—considerably less than that expected from Ekman's (1905) wind-driven flow model. These observations are in good agreement with all the previous NORPAX drifter observations in the midlatitude North Pacific during the fall–winter seasons (McNally, 1981), after they were corrected for windage. Moreover, they are consistent with the very observations which led to Ekman's work, namely those of Nansen (1902) of polar ice drift with respect to the surface wind which Sverdrup (1931) reported indicated drift 29° to the right of the wind at 1.67% of the wind speed.

The greater significance of windage cited in this study is directly attributable to the smaller size of the drogues used. Recall that when these present data were corrected for windage the angle between the drifter displacements increased from ~17° to the right of the wind to ~30° to the right of the wind. McNally (1981) cited the same 30° angle thus supporting the conclusion therein that windage was not a significant factor in these earlier deployments. We now conclude that this was due to the large size of the standard drogues.

On the other hand, this increase in windage incurred by decreasing the drogue size is inconsistent with the reported lack of a statistically significant difference in behavior of drogued and undrogued drifters also reported in McNally (1981). Since we as yet do not know the mechanism responsible for the nonwindage portion of the downwind velocity, it is possible that the abnormal atmosphere forcing (three times the standard deviation of the climatological norm in the region) might have resulted in an overwhelmingly larger nonwindage component. However it is more likely that the use of displacements (i.e., integrated velocities) in the present study provides an enhancement of the windage effect which was not true of the methodology used on the earlier study; ensemble averages of 5-day running mean daily wind on drifter velocity vectors.

The basic similarity in the behavior of all the drifters (Figs. 1 and 2) made it possible to examine in detail only one of the four drifter groups, namely that deployed at 37°N.

The multi-drogued depths employed in this deployment provided the necessary observations to confirm the hypothesis suggested by previous drifter deployments in this region (McNally, 1981) that the wind-driven flow was uniform with depth in the mixed layer. Different drogue depths and seasonal deeping of the mixed layer combine to provide observations in September and October of the flow both within and beneath the mixed layer. The transition of a drifter's drogue from beneath the mixed layer to within the mixed layer was shown to be characterized by a coincidental appearance of large near-inertial motions (Fig. 4) and the onset of persistent downwind and crosswind displacements (Fig. 3), with the downwind component three times larger than the crosswind. The similarity of the displacements of the 30-, 60-, and 90-meter drogued drifters, subsequent to the entry of their drogues into the mixed layer, demonstrated that the wind driven flow was uniform throughout the mixed layer.

It was hypothesized that drifter observations in the mixed layer were the result of a combination of Ekman slab flow, directed 90° to the right of the surface wind stress, and windage (i.e. downwind motion directly forced by the wind drag acting on the exposed portion of the drifter hull). A model was constructed for each of these mechanisms. The windage model assumed a static balance of forces. The displacements (Fig. 7, right panel) constructed from the residual downwind and crosswind velocities, obtained by subtracting the model velocities from the observed, show the Ekman slab model accounting for up to 80–90% of the observed crosswind displacement. On the other hand, the windage model was not very successful, accounting for ~40% of the observed downwind displacement. Cross-correlation of 6-hourly wind stress values with the residual downwind velocities (i.e., after subtracting the windage estimate) shows the downwind residual velocity to have lagged the wind stress by 6 to 12 hours, exhibiting a "memory" of up to 1.5 days. The generating mechanism for this downwind component of mixed layer motion that lags the wind remains unexplained.

Recently, Davis *et al.* 1982 reported on the results of a laboratory study of the behavior of models of drifter hulls of different designs in a wave tank. This report identifies another possible mechanism that could produce a systematic bias in a drifter displacements, "waveage." Waveage is incurred as a result of a drifter's hull failure to provide the same wetted drag area to the orbital velocity field of the surface waves. The dynamic response of a hull to surface wave forcing coupled with a nonsymmetric hull can combine to rectify the orbital velocities so as to produce a net displacement when there is zero mean flow. Further, Davis *et al.* report that the direction of this displacement can be either up or downwave depending on a hull's response characteristics. The degree that phenomena affects the behavior of the drifter type under discussion, with their large rather deep drogues is unknown. However, neither windage or waveage, or some combination thereof is consistent with the the behavioral change incurred by these drifters when their drogues entered the mixed layer. The sudden onset of persistent downwind and crosswind displacements can not be attributed to either windage or waveage.

Drifter observations of the flow beneath the mixed layer are confined to the 60-meter drogued drifter in September and the 90-meter drogued drifter in September and October. Residual displacements of these drifters during these periods indicate displacements which rotate counterclockwise to the left of the wind into the downwind direction when the drogues entered the mixed layer (Fig. 7). A plot of 5-day averaged downwind–crosswind residual velocities (Fig. 5) suggests a wind driven flow beneath the mixed layer, whose amplitude decreases and whose direction turns in a clockwise sense further to the right of the surface wind with increasing depth. A detailed analysis of this flow is not possible because of incomplete data on mixed layer deepening available from the TRANSPAC XBT data and the lack of a precise knowledge of the actual drogue depth.

Acknowledgments. We wish to thank the Captain and crew of the R/V *New Horizon* for their cooperation in the deployment of these drifters and John McGowen who graciously made time and space available on his cruise for the deployment. We would also like to thank Ms. E. Barnier for her patience in typing the many revisions of the manuscript. Finally we are pleased to acknowledge the Office of Naval Research who, under Contract USN N00014-80-C-0440, provided the necessary support for this work.

REFERENCES

Davis, R. E., J. E. Defour, G. J. Parks and M. R. Perkins, 1982: Two inexpensive current following drifters. Ref. No. 82-28, Scripps Institution of Oceanography.

——, R. de Szoeke and P. Niiler, 1981: Variability in the upper ocean during MILE. Part II: Modeling and mixed layer response. *Deep Sea Res.*, **28A,** 1453–1475.

Defant, A., *Physical Oceanography, Vol. 1,* MacMillan, 1961.

Ekman, V. W., 1905: On the influence of the earth's rotation on ocean-currents. *Ark. Mat. Astron. Fys.*, **2,** 1–53.

Fissel, A., S. Pond and M. Miyaki, 1977: Computation of surface fluxes from climatological and synoptic data. *Mon. Wea. Rev.*, **105,** 26–36.

Friehe, C., and S. Pazan, 1978: Performance of an air-sea interaction buoy. *J. Appl. Meteor.*, **17,** 1488–1497.

Kirwan, A. D., Jr., G. McNally and S. Pazan, 1978a: Wind drag and relative separations of undrogued drifter. *J. Phys. Oceanogr.*, **8,** 1149–1153.

——, ——, E. Reyna and W. J. Merrell, Jr., 1978b: The near surface circulation of the eastern North Pacific. *J. Phys. Oceanogr.*, **8,** 937–945.

——, ——, S. Pazan and R. Wert, 1979: Analysis of surface currents response to wind. *J. Phys. Oceanogr.*, **9,** 401–412.

McNally, G. J., 1981: Satellite-tracked drift buoy observations of the near-surface flow in the eastern mid-latitude North Pacific. *J. Geophys. Res.*, **86,** 8022–8030.

——, E. Reyna, W. J. Merrell, Jr. and A. D. Kirwin, Jr., 1978. Technical evaluation of ADS I and ADS II drifter performance. Rep. 78-3-T, Texas A&M University.

Nansen, F., 1902: Oceanography of the North Polar Basin, The Norwegian North Polar Expedition (1893–96). *Sci. Results.*, **3.**

Price, James F., 1983: Internal wave wake of a moving storm. Part 1: Energy budget and observations. *J. Phys. Oceanogr.*, **13,** 949–965.

Sverdrup, H. U., 1931: The wind drift of the ice on the North Siberian Shelf, North Polar Expedition "Maud" 1918–1925. *Sci. Res.*, **6,** 131–175.

White, W. and R. Bernstein, 1979: Design of an oceanographic network in the midlatitude North Pacific. *J. Phys. Oceanogr.*, **9,** 592–606.